

REVIEW

Investigation of the Some Electron Transfer Bioprocesses by Voltammetric Techniques

I. G. DAVID*, M. DIACONU**, G. L. RADU***, V. DAVID*

*Department of Analytical Chemistry, Faculty of Chemistry, University of Bucharest

** Department of Analytical Biochemistry, National Institute for Biological Sciences

*** Centre of Research in Enzymology, Biotechnology and Bioanalysis, University of Bucharest

Received 10th November, 2001; Accepted 5th January, 2002

Abstract

This paper is an overview on the electrochemical techniques employed in the investigation of electron transfer reactions of biological important compounds at different types of electrodes (mercury or solide electrodes, bare or modified electrodes). We have selected for exemplification, only cytochrome and superoxide dismutase from a large variety of substances of with biological significance participating to electron transfer processes. These processes involve either non-mediated or mediated bioelectrocatalysis. The voltametric technique most often used in this purpose was CV but also some polarographic techniques (DCP, oscillopolarography) were employed. The development of different types of sensors was a direct applicability of such studies.

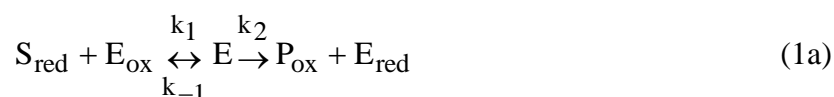
Keywords: transfer charge bioprocess, bioelectrochemistry, bioelectrocatalysis, cytochrome c, superoxide dismutase

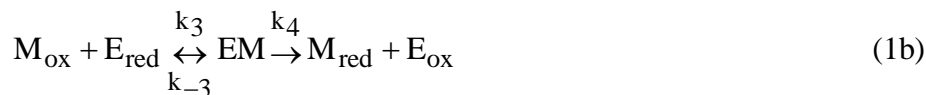
Introduction

Nowadays, an important trend of bioelectrochemistry is the study of mediated and non-mediated bioelectrocatalysis where enzymes interact directly with electrodes.

In mediated bioelectrocatalysis reactions [1] different enzyme reactions can be coupled with electrode reactions of redox compounds - called electron transfer mediators - which shuttle electrons between the enzymes and the electrodes. This reaction system is useful to design biosensors and bioreactors, to amplify mediators detection and to measure enzyme kinetic and protein redox potentials.

The electron flow in mediated bioelectrocatalysis can be represented as in **Figure 1** and equations 1(a) and 1(b)





where S and P are the substrate and product, E_{ox} and E_{red} are the oxidised and reduced forms of the enzyme and M_{ox} and M_{red} are an electron acceptor and its reduced form, respectively; k₁, k₋₁, k₂, k₃, k₄ are the rate constants of the respective steps. The steady-state kinetics of the enzyme reaction (v_E) is:

$$v_E = \frac{k_{cat} [E]}{1 + \frac{K_M}{[M_{ox}]} + \frac{K_S}{[S]}} \quad (2)$$

where [E] is the enzyme concentration, k_{cat} = k₂k₄/(k₂ + k₄) is the catalytic constant and K_M = k₂(k₋₃ + k₄)/k₃(k₂ + k₄) and K_S = k₄(k₋₁ + k₂)/k₁(k₂ + k₄) are the Michaelis constants of M_{ox} and S, respectively.

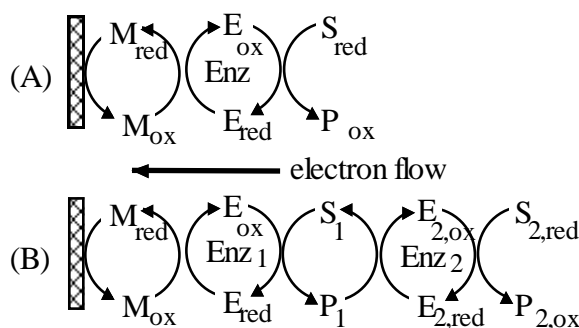


Figure 1. Kinetic scheme of mediated bioelectrocatalysis in (A) one-enzyme and (B) two-enzyme-linked systems.

On the other hand M_{red} and M_{ox} undergo an electrode reaction:



where n is the electrons number and k and k are the electron-transfer rate constants. According to **Figure 1**, M_{ox} is generated electrochemically at suitable electrode potentials (E) (eq. 3) and incorporated in the enzymatic reaction (eqs. 1(a) and 1(b)).

Cyclic voltammetry was often used for the study of an electrochemical reaction coupled with a mediated enzyme reaction in order to explore reaction kinetics. **Figure 2** presents cyclic voltammograms of homogeneous mediated bioelectrocatalysis where M_{ox} and M_{red} are reversible (curve A). If the bulk concentration of the substrate ([S]^{*}) is sufficiently larger than K_s and the bulk concentration of M_{red} ([M_{red}]^{*}) is smaller than K_M a typical sigmoidal catalytic wave can be observed (curve C). At lowered [S]^{*} the voltammogram

shows no steady-state current due to the substrate depression near the electrode surface (curve B). At increased $[M_{\text{red}}]^*$ an anodic peak of the diffusion current of M_{red} is overlapped on the catalytic current but the current becomes steady state after suitable periods at high $[S]^*$ (curve D) [2].

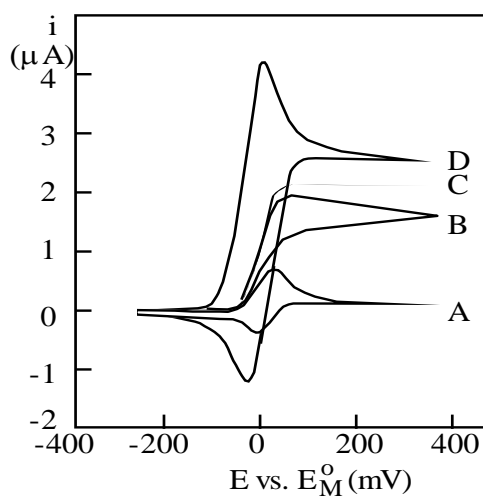
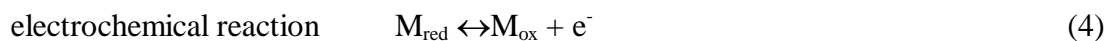


Figure 2. Cyclic voltammograms representing homogeneous mediated bioelectrocatalysis (A) M_{red} alone ($n=1$, totally reversible case) (B) - (D) $M_{\text{red}}+E+S$ $[M_{\text{red}}]^*=0.1$ mM (D: 2 mM), $[S]^*=100$ mM (B:0.7 mM), $k_{\text{cat}}[E]=1$ mM s^{-1} (D: 0.1 mM s^{-1}); $K_M=1$ mM, $K_S=1$ mM, $A=0.1$ cm^2 (D: 0.01 cm^2); $v=10$ $mV s^{-1}$.

Several researchers have tried to simulate of the mediated enzyme electrochemistry [3-16]. A cyclic voltammetric simulation applied to an electrochemically mediated enzyme reaction involving any substrate and any mediator concentrations has developed [17]. Both, the concentration polarisation of the substrate in the electrode vicinity and the mediator concentration were considered. Reversible and quasi-reversible one electron electrochemical reactions followed by a two electron enzyme reaction schema was proposed, according to the following:



where M_{red} , M_{ox} , S and P are the reduced and oxidized form of the mediator, substrate and product, respectively. The electrochemical reaction takes place at the electrode surface with full reversible kinetics and the enzyme reaction occurs in the solution.

The differential equations for mediator and substrate were solved using a digital simulation technique. The calculated cyclic voltammograms present pre-peaks when there was low substrate concentration, high mediator concentration and high enzyme activity. The shape of the voltammograms changes as these values are modified. **Figure 3** shows calculated cyclic voltammograms at four mediator concentrations and three different enzyme activities. These curves demonstrate that the pre-peak is observed at both high mediator concentration and high enzyme activity. This is due to the depletion of the substrate concentration.

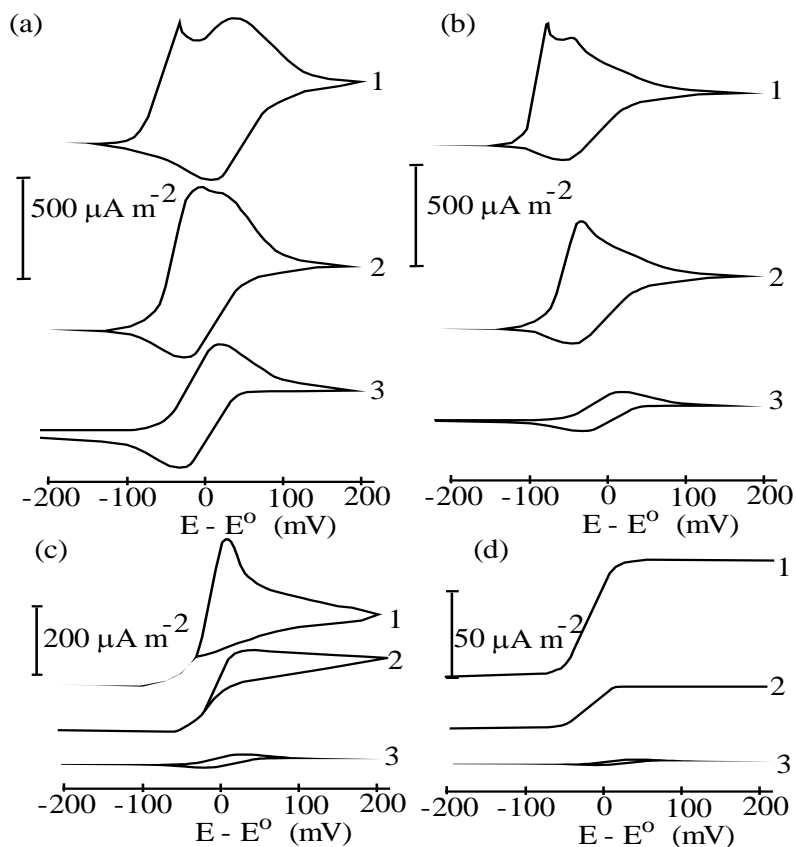


Figure 3. Calculated cyclic voltammograms of reversible electrochemistry coupled with a homogeneous enzyme reaction. $v=1 \text{ mV s}^{-1}$, $C_S^*=10 \text{ mM}$, $D_{M_{\text{red}}}=D_{M_{\text{ox}}}=D_S=5 \cdot 10^{-6} \text{ cm}^2 \text{ s}^{-1}$, $K_{MM}=1 \text{ mM}$, $K_{MS}=1 \text{ mM}$, $C_{M_{\text{red}}}^*=(a) 20, (b) 10, (c) 1 \text{ and } (d) 0,1 \text{ mM}$, $k_{\text{cat}}C_E=(1) 10, (2) 1 \text{ and } (3) 0 \text{ mM s}^{-1}$. (C_S^* and $C_{M_{\text{red}}}^*$ are the bulk concentrations of M_{red} and S).

Digital simulation was applied to the determination of the kinetic constants k_{cat} , K_{MM} , K_{MS} of glucose oxydase (GOx). CV was carried out experimentally in phosphate buffer solution containing GOx, ferrocene derivatives (ferrocenemethanol, 1, 1'-ferrocenedimethanol and (ferrocenylmethyl)trimethylammonium (FMTMA) perchlorate) and glucose. A good agreement was observed between the simulated and the experimental cyclic voltammograms after baseline compensation at several substrate concentrations.

Enzyme kinetic constants were determined from the current values obtained by simulation and experimentation. The k_{cat} , K_{MM} and K_{MS} values for GOx, 1, 1'-ferrocenedimethanol and glucose were 340 s^{-1} , 110 μM and 30 mM , respectively [17].

For many years much attention has been paid to the electrochemical behaviour of proteins at mercury electrodes. A large number of papers and several reviews on the proteins adsorption and the reduction of disulphide bonds on mercury electrodes have been reported [18-23].

CYTOCHROMES

As is well known, the formal potentials of redox proteins are very useful to understand the biological reactions in which they may be involved as electron carriers. Voltammetric techniques using macroelectrodes proved to be valuable tools in the supplying of experimental data. However, meaningful thermodynamic potentials of metalloproteins require firstly a thorough analysis of the electrochemical results. Marked changes in potential may occur due

to, e.g. adsorption phenomena and the degree of reversibility of the electrode processes [24].

Cytochrome c (cyt c) is a water soluble hem metalloprotein playing an important role in the biological respiratory chain. It receives electrons from the cytochrome c reductase and deliver them to cytochrome c oxydase [25].

In *in vivo* conditions, cytochromes are part of the energy conserving electron transport system. They have a protoheme prosthetic group covalently attached by two thio ether bridges between the cysteine residues of the protein and the vinyl side chains of the hem. Mammalian peroxidases and type c cytochromes are the only hemoproteins with a covalently bound hem group. The location and the role of mitochondrial cyt c are well known but the means by which cyt c conducts electrons between its membrane reductase and oxydase remains controversial. But there exist arguments for the diffusion of cyt c across the membrane surface to interact separately with its reductase and oxidase. Cyt c is a protein ubiquitous to all eukaryotic organisms and the sequence of many such proteins have been determined.

Cyt c used as a biocatalyst presents [26] some advantages:

1. the hem prosthetic groups is covalently bound to protein. This property may be important for catalysis in the presence of organic solvents, cyt c does not lose its hem catalytic group in these systems, while peroxidase do;
2. cyt c is active over a wide range of pH;
3. biocatalytic activity was found at high concentrations of organic solvents
4. horse heart cyt c is able to perform biocatalytic reactions at higher temperatures than 120°C with a maximum activity at 80 °C (after chemical modification, its thermostability could be greatly increased);
5. cyt c is inexpensive, cost and stability are two main factors for biocatalysis in a large scale.

Electrochemistry of metalloproteins is a subject of great interest. Among other things it helps in understanding the requirements for rapid and reversible electron transfer between a soluble protein and the electrode surface and it constitutes a good approach to redox processes taking place *in vivo* [27, 28].

Generally, metalloproteins are electrochemically inert at bare electrode surfaces because of (I) the inaccessibility to the active site, often buried in a crevice provided by a polypeptide chain and (II) the lack of recognition of the surface patch involved in complex formation and electron transfer with a biological partner. As a consequence, electron transfer of redox proteins, which is often very fast, becomes extremely slow at an electrode surface, thereby hindering detection of signals when conventional electrochemical techniques are employed [29].

The electrochemistry of several c-type cytochromes at a variety of electrode surfaces emphasised that the electrode reaction of cyt c at bare metal electrodes, such as mercury [30-34], platinum [35], gold [36] and silver [37] is significant irreversible. Rapid electron transfer reactions of cyt c can be achieved by addition of promoters to the solution [38, 39] or by modifying the electrode surfaces [40-44]. Promoters are chemicals possessing functional groups interacting with the protein and thus inducing an orientation of the macromolecule favourable for rapid electron transfer; they are not like conventional mediators because although such a compound encourages electron transfer with the protein to proceed, it does not take part in the electron transfer process being electrochemically inactive in the potential range of the investigated redox process [45]. Promoters can be directly adsorbed on the electrode surface [46] or fixed to it after entrapment into a solid matrix [47,48]. Quasi-reversible cyclic voltammograms for cyt c at metal oxides [49,50] and graphite electrodes in the edge plane have also been reported.

Electrochemical studies of cyt c at mercury electrodes outlined the fact that in such systems the adsorption phenomena plays an important role which in most cases produces denaturation of the protein [51]. Therefore, mercury with some exceptions has no longer been widely used in electrochemistry of proteins and it has been recognised as being largely incompatible with biological molecules [45]. Competitive adsorption between a promoter and the protein is an important factor to prevent conformation changes in the protein with loss of electron transfer activity. Other studies have investigated the adsorption and chemical reactions of the protein at a mercury electrode covered by a monolayer of 4, 4'-bipyridyl [52]. There takes place both the displacement and the rearrangement of the electron carrier bipyridil, forming the first layer, due to the completely irreversible protein adsorption process. Other proteins also adsorb irreversible on the Hg electrode in the presence of bipyridyl. As a consequence of the competence of the bridge of the electron carriers and the protein adsorption, the useful potential range for promoting electron transfer of protein at electrodes is significantly narrower for the mercury than for the gold substrate.

In spite of these disadvantages to a bridge electron carrier for promoting reversible electron transfer of macromolecules, the other characteristics of mercury, as a liquid metal, make it an ideal substrate to study the properties of adsorbed monolayers, which are apparently independent of the crystal lattice surface [53].

The very high affinity of mercury for thiol groups facilitates the protection of the surface with an adsorbed organic monolayer, which acting as a promoter, compares quite well to the reversible exchange of the protein in gold or other metal-modified interfaces. Thus the mercury surface was also modified by the chemisorption of a 6-mercaptopurine (6MP) self-assembled monolayer (SAM) [54].

The cyclic voltammograms recorded for a cyt c solution in 0.1 M acetate buffer (pH 6.0) at both at a 6MP modified hanging mercury drop electrode (HMDE) and a 6MP modified gold electrode (**Figure 4 b, c**) present a couple of well defined peaks attributed to the electron transfer reaction of cyt c at the modified electrodes in which 6MP acts as a promoter. The signal is due to cyt c since 6MP (**Figure 4 a**) does not exhibit an electrochemical response in this potential range. On the other hand no response is obtained at a bare mercury electrode for the same protein solution.

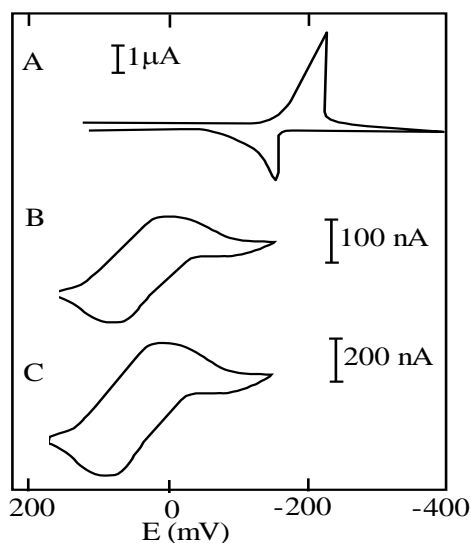


Figure 4 - Cyclic voltammograms at 6MP-modified electrodes in 0.1 M acetic buffer (pH 6.0). (a) 6MP-HMDE in blank solution; (b) 6 MP-HMDE in solution containing 460 nM cyt c; (c) 6 MP-gold electrode in solution (B). Scan rate 100 mV s⁻¹ for (A) and 20 mV s⁻¹ (B) and (C).

The ratio of the anodic to cathodic peak currents I_{pa}/I_{pc} remains constant and close to the unity when the scan rate is modified whereas both cathodic and anodic peak currents vary linearly with $v^{1/2}$ which confirms the diffusion controlled redox process of cyt c. The estimated diffusion coefficient ($D_o = 7.7 \cdot 10^{-7} \text{ cm}^2 \text{ s}^{-1}$) value is similar to those reported for other promoters [21, 44, 55-58].

The separation between the cathodic and the anodic peaks indicates a quasi-reversible one-electron transfer reaction. The midpoint between the anodic and cathodic peak potentials representing the redox potential of c type cytochromes is influenced by two salt-induced effects, namely the changes in the activity coefficients of both redox states and specific anion binding to protein surface sites. The first effect is related to the stabilisation of the oxidized state of cyt c over the reduced one, leading to a decrease of the redox potential with increasing ionic strength. The other effect, is due, besides the general ionic strength effect, to the ionic composition of the medium that results in an additional decrease of $E^{o'}$ trough specific anion bindings to the surface sites with low or high affinity. It seems that the potential shift has no relationship with the substrate type (i. e. Hg or Au).

The stability of the modified electrode was examined by continuous scanning. In contrast with studies of other promoters where changes occur after successive scans the stability of the 6MP coated electrodes is ascribed to the high affinity of the S by the metal in SAM with either mercury or gold.

The redox exchange of the protein with the coated mercury electrode is a function of the excess of surface coverage of 6MP promoter.

At a 6 MP coated HMDE one can obtain promoted quasi reversible stable electrochemistry of cyt c. The formal redox potential $E^{o'} = 5 \text{ mV}$ (vs. SCE), the diffusion coefficient ($D = 7.7 \cdot 10^{-7} \text{ cm}^2 \text{ s}^{-1}$), the formal heterogeneous electron transfer rate constant $k_o = 4.1 \cdot 10^{-3} \text{ cm s}^{-1}$ and the transfer coefficient $\alpha = 0.5$ obtained for cyt c at a 6MP-HMDE are practically the same with those obtained at the 6MP modified Au electrode and they are in agreement to those reported for the native protein [44, 45 58, 59].

Eddows and Hill were the firsts that obtained reversible cyclic voltammograms of horse heart cyt c employing a 4, 4'-dipyridil modified gold electrode [39, 60]

Hill's group used in their further investigations gold electrodes modified by adsorption of small organic compounds [61], including small peptides [62] and amino acids together with some derivatized molecules [63]. Direct electrochemistry of horse heart cyt c was also investigated in the presence of different amino acids [64] and at polymer [65] modified electrodes.

Santucci et al [66] have compared the electrochemical behaviour of cyt c and microperoxidase (**Figure 5**) at

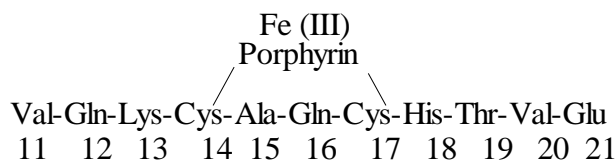


Figure 5. Chemical structure of microperoxidase, the heme-peptide obtained by hydrolysis of cytochrome c. The number refer to the amino acid sequence in the native protein.

gold electrodes chemically modified by absorption with sulphur containing compounds and well shaped quasi-reversible diffusion-controlled cyclic voltammograms were obtained for all compounds except cysteine which exhibits poorly defined waves. The experimental results Roum. Biotechnol. Lett., Vol. 7, No. 2, 603-624 (2002)

(table 1) indicate that the electroactivity of cyt c depends on the type of promoter used. The order of efficiency displayed by the different promoters is cysteine>N-acetylcysteine>cysteine ethyl ester>diformyl cysteine>>cystine (very low promotion). Microperoxidase behaves differently from cyt c undergoing a more rapid electron transfer at a chemically modified electrode and the electron transfer are favoured by promoters providing positively charged groups (e.g. cysteine ethyl ester) while for cyt c electroactivity is favoured by negatively charged groups (e. g. N-acetylcysteine). In the case of microperoxidase the promoter efficiency decreases in the order cysteine ethyl ester>cysteine>diformyl cysteine>>cysteine (irreversible cyclic voltammograms obtained)>n-acetyl cysteine (no promotion).

Table 1. Thermodynamic and kinetic parameters for heterogeneous electron transfer of cytochrome c and microperoxidase at a chemically modified gold electrode

Modifier	Cytochrome c ^a			Microperoxidase ^b		
	ΔE_p /mV	$E_{1/2}$ /mV (SHE)	$10^3 k_s$ ^c / cm s ⁻¹	ΔE_p /mV	$E_{1/2}$ /mV (SHE)	$10^3 k_s$ ^c / cm s ⁻¹
Cysteine	82	255	3.2	87	-160	3.2
N-acetylcysteine	85	255	2.3	-	-	-
Cysteine ethyl ester	90	264	2.0	75	-160	6.1
Cystine	-	-	-	-	-	-
Diformyl cysteine	96	260	1.6	95	-160	2.4

Experimental conditions: 20 mM phosphate buffer (pH 7.0) plus 100 mM NaClO₄, as supporting electrolyte; ^a scan rate 50 mV s⁻¹; ^b scan rate 100 mV s⁻¹; ^c values estimated on the basis of n=1, $\alpha=0.5$ and T=25 °C.

The essential factors favouring rapid reversible heterogeneous electron transfer at a chemically modified gold electrode are the electrostatic interactions between the promoter and the diffusing hem carrier molecule and the molecular architecture of the promoter.

Compared with microperoxidase (where the hem is almost completely exposed to the solvent) cyt c displays excellent electrochemical behaviour despite the low accessibility of the hem buried in a crevice provided by the polypeptide chain. The data from **Table 1** indicate that, where a comparison is possible, the two systems behave similarly. The data also suggest that the pathway(s) of the electron in homogeneous and heterogeneous electron transfer may be the same.

The electrochemical behaviour of cyt c was also investigated by CV on a gold electrode modified by self-assembly immobilisation of double-stranded, thiol-modified oligonucleotides forming a thin layer [67]. These films proved to be efficient promoters for fast electron transfer and showed a good adsorption capability for cyt c which was also found to be reversible. Thus, cyt c was investigated both immobilised and in solution showing reversible electrochemical behaviour in each case. It was demonstrated (linear dependence of I_p on $v^{1/2}$) that the surface reactions were diffusion controlled rather than by adsorption and the anodic and cathodic peak currents vary linear with cyt c concentration in solution in the range 20-200 μ M.

In contrast to mercaptoalkanoic acid (n>9) modified electrode the surface reaction at oligonucleotide modified electrode appears to be more reversible. This behaviour was attributed to the modification by thiol chemisorption since a non-thiol modified oligonucleotide showed only weak adsorption at the gold electrode and resulted in a weak or poorly defined electrochemical behaviour of cyt c.

Cyclic voltammograms recorded for cyt c at a bare glassy carbon electrode (GCE) in phosphate buffer present two well defined redox peaks that appear near the thermodynamic redox potential ($E_{1/2}=0.245$ V vs. SCE) [68]. Cyt c in its native form is not strongly adsorbed

at the GCE surface and gives a reversible diffusion-controlled redox process.

The voltammetric behaviour of cyt c depends strongly on the surface state of the GCE. Freshly polished GCE surface possesses a number of C-O groups as suitable sites for direct electrochemical reaction of cyt c facilitating the direct electron transfer.

The adsorption of cyt c on the GCE, which increases when the immersion time increased, may produce changes in the surface state of the electrode (e.g. deactivation or fouling) resulting a modification of the electrochemical behaviour of cyt c. The adsorption of cyt c on GCE surface decreases the electron transfer rate more than other contaminants.

Direct electrochemical behaviour of cyt c cannot be observed at the nafion-modified GCE when cyt c is strongly adsorbed by electrostatic interaction on the Nafion film.

Cyclic voltammograms of cyt c recorded at a GCE covered with a microporous alumina membrane [69] are different from those obtained at a bare GCE, both the cathodic and anodic peaks being much better defined in the former case. The analysis of these voltammograms indicate that a large conformational change or a denaturation does not occur at the alumina membrane-covered GCE. Thus, the alumina membrane seems to be a "solid-state" promoter for cyt c.

The good agreement between experimental and simulated curves indicates that the electrochemical reaction of cyt c at the GCE covered with an alumina membrane is described by a standard semi-infinite diffusion process.

Correia dos Santos et al. [24] have performed a study of unmediated electrochemistry of redox proteins on three c-type cytochrome at inlaid disk microelectrodes of Pt, Au and C employing linear scan, differential pulse and square wave voltammetry. In all experiments the promoter 4,4'-dipyridyl was used. For comparison the electrochemical behaviour of the three compounds was evaluated in terms of kinetics. The reduction of cyt c₅₅₃ from *D. Vulgaris* at both micro and macro Pt, Au and C electrodes is reversible. The same behaviour presents cyt c at a Pt microelectrode though the reduction at a Au microelectrode occurs at the boundary of reversibility [24] and that at Pt, Au and C macroelectrodes is quasi-reversible. The analysis of steady state voltammograms of cyt c₅₅₂ from *P. nautica* suggests also a quasi-reversible behaviour.

The values of the heterogeneous rate constants determined at both macro and microelectrodes for cyt c₅₅₂ and horse heart cyt c were in good agreement.

The diffusion coefficients of the monohemic cytochromes were evaluated from voltammetric data at microelectrodes and have values around $1 \cdot 10^{-6} \text{ cm}^2 \text{ s}^{-1}$. No literature values were known for comparison but since the molar masses of all the three cytochromes are alike, similar diffusion coefficients are expected.

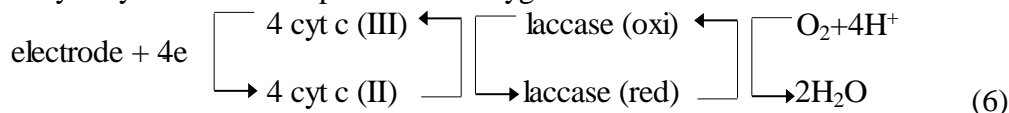
A wide range of redox potential was obtained for the studied hem proteins. The redox potential of cyt c₅₅₃ is more negative than those of other class member. Since the redox potential of a cytochrome is the result of multiple contributions (electrostatic and hydrophobic environment of the hem pocket, hydrogen bonding, hem axial ligands, geometry, solvent exposure etc.) and assuming that the main overall structural features are maintained within these cases it may be observed the result of a very fine tuning of the hem environment in the redox properties. It was proposed a correlation between the length of the Fe-S bond and the redox potential of monohem cytochromes with methionine-histidine coordination. The shorter the Fe-S bond is the more negative is the potential but this proposal has no further scientific support.

Immobilised cyt c was also investigated with respect to its reaction with species present in solution. Superoxide radicals rapidly reduce cyt c oxidised. Thus, there are small effects because the small superoxide concentration due to the short lifetime of the radical in aqueous

solution. It could be confirmed that the electroactive and immobilised cyt c is still accessible at least for small analyte molecules.

The electron transfer between cyt c and structurally closely related multicopper oxidases (ascorbate oxidase or laccase from *Coriolus hirsutus*) was investigated on a gold electrode modified with 4, 4'-dithiopyridine when cyt c exhibits a quasi-reversible one-electron cyclic voltammogram [71]. The peak current increased linearly in the concentration range 50-800 μM cyt c.

After addition of laccase to the cyt c solution a sigmoidally shaped voltammogram appears and the current increases due to the catalytic regeneration of ferricythochrome c in the diffusion layer by laccase in the presence of oxygen in accordance with the following reaction:



The electron transfer reaction of laccase with cyt c is a second order process:



The second order rate constant of electron transfer reaction between laccase and other copper proteins can be as high as $10^7 \text{ M}^{-1} \text{ s}^{-1}$. The natural electron acceptor of cyt c in the respiratory chain is the 160kD hem copper enzyme cythochrome c oxidase. It contains two cythochromes (a and a₃) and two copper atoms per molecule (CuA and CuB). The reaction with ferrocycytochrome c starts at the cyt a with a homogeneous rate constant of the order (8-9) $10^6 \text{ M}^{-1} \text{ s}^{-1}$. Laccase substitutes the function of cyt c oxidase by mediating the oxidation of cyt c at the expense of oxygen.

Similar studies with other copper enzymes (ascorbate oxidase, ceruloplasmin and tyrosinase) showed that these compounds are also capable to oxidise cyt c. The order of the reaction rate with cyt c is laccase > tyrosinase > ascorbate oxidase > ceruloplasmin. The difference in the redox potential is considered to be the driving force of the reaction of cyt c and the copper proteins investigated. The kinetics of the redox process is also influenced by the protein size and the electrostatic interactions.

Lojou et al. had used CV to investigate the kinetics of electron transfer between several types of polyheme c-type cytochromes and soluble Fe(III) complex [72] and various soluble or solid metal oxides [73]. The second order rate constants calculated were situated for the Fe(III) complex reduction in the 10^5 - 10^6 M s^{-1} whereas that for the reduction of soluble chromate was of the same order of magnitude, namely $6 \cdot 10^5 \text{ M s}^{-1}$. Cyt c₇ also acts as Mn(IV)-, V(V)- and Fe(III)-oxide reductase. This activity however depends on the oxide form. Due to the ability of the Eastman AQ polymers [poly (ester sulphonic acid) ionomer] to entrap positively charged cytochromes was demonstrated that the immobilisation of the cytochromes in the polymer matrix does not inhibit the electrocatalytic process.

The result had suggested that the metal reductase activity of a microorganism is governed by its c-type cytochrome content. Furthermore, only cythochromes with bihistidiny hem iron coordination act as metal reducers whereas mitochondrial c-type cyt do not.

Processes involving the use of entrapped enzymes reactions could be developed according to the metal reducing activity of their polyheme c-type cytochromes.

CV at a GCE and direct current polarography (DCP) were employed to demonstrate the catalytic properties of cyt c in the electroreduction of the nitric oxide produced by the disproportionation reaction of nitrite [74]. The addition of NaNO_2 to a buffer electrolyte solution did not cause an observable change in the shape of the voltammogram but if a small amount of cyt c was also added, a large cathodic wave appeared with the peak potential at -

0.58 V accompanied by a very small preceding wave at -0.1 V which was attributed to the reduction of a trace amount of oxygen in the solution.

DCP emphasised also that when cyt c is added to a nitrite solution a cathodic wave appears, starting from -0.5 V as observed by CV with CGE.

SUPEROXIDE DISMUTASE (SOD)

SOD, an enzyme that catalyses the superoxide radical dismutation to H_2O_2 was discovered in 1968 [75]. SOD plays a major protective role in living cells and has been widely used as a pharmacological tool in the study of pathophysiological mechanisms [76-79]. The ubiquitous presence of SOD enzyme throughout the evolutionary chain emphasises the importance of the superoxide radical in cell function and survival. Superoxide radical (O_2^-) is highly reactive and short-lived and is formed in all aerobic cells. The superoxide radical generated during the "respiratory burst" of phagocytic cells plays an important role in the destruction of microorganisms invading into the body. But it may be involved in oxidative damage to tissues and organisms if it exceeds the level at which the systems are able to provide defence. Under normal pathological conditions, the highly reactive superoxide radical undergoes disproportionation by non-catalytic and enzymatic reactions; thus the physiological concentration is rather low ($\sim 10^{-11}$ M). The superoxide radical is linked with a number of diseases and the diagnosis of these diseases is currently performed by the superoxide radical detection.

Analytical methods for the determination of SOD are based on its ability to accelerate the dismutation of O_2^- and require a source of superoxide ion and a system for detecting it.

Detection of superoxide and SOD has been intensively investigated by spectrometric and electrochemical methods [59, 63, 80-86]

Copper-zinc superoxide dismutase Cu_2Zn_2SOD (porcine superoxide dismutase PESOD) is an important enzyme with defence functions which contains two identical subunits each containing one copper (II) and one zinc(II) ion which are connected by a histidine imidazolate bridge.

For the first time, the electrochemical behaviour of PESOD at mercury electrodes was investigated by CV and DCP in the absence of mediators. It is abnormal that PESOD displays two pairs of redox irreversible adsorbed peaks ($E_{pc1} = -0.71$ V, $E_{pa1} = -0.647$ V, $E_{pc2} = -1.026$ V, $E_{pa2} = -0.945$) in the CV diagram (**Figure 6a**).

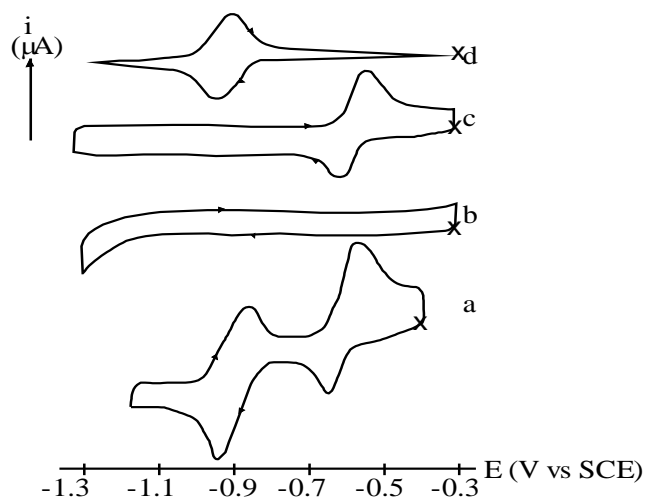


Figure 6. Cyclic voltammogram of PESOD and derivatives of PESOD on HMDE, scan rate 0.10 V s^{-1} , (a) PESOD ($9.56 \cdot 10^{-5} \text{ M}$); (b) $\text{E}_2\text{E}_2\text{SOD}$; (c) $\text{Cu}_2\text{E}_3\text{SOD}$; (d) $\text{E}_2\text{Zn}_2\text{SOD}$; concentration of all SOD derivatives is $1 \cdot 10^{-4} \text{ M}$; Supporting electrolyte: 0.01 M phosphate buffer + 0.1 M KCl, pH 7.4.

The ratios of the cathode to anode current was close to the unit for both peak pairs and the potentials separations of the anodic and cathodic peaks ($\Delta E_1=63 \text{ mV}$ and $\Delta E_2=81 \text{ mV}$) that were independent on the scan rates indicate a quasi-reversible electrode process. The straight line of the plot I_p vs. scan rate showed that the process posses adsorptive characteristics under CV conditions. It was demonstrated that the PESOD adsorption on the electrode surface was irreversible by the peaks persistence for several minutes on the CV diagram recorded after washing and transferring the electrode into pure supporting electrolyte.

These peaks are located in the potential regions of the disulphide bonds of many proteins but they were attributed to the redox peaks of Cu(II) and Zn(II) by PESOD reconstitution (**Figure 6**). The CV diagram of $\text{E}_2\text{E}_2\text{SOD}$ (**Figure 6b**) present no redox process in the investigated region. Comparing the CV diagram of $\text{Cu}_2\text{E}_2\text{SOD}$ (**Figure 6c**) with that of $\text{Cu}_2\text{Zn}_2\text{SOD}$ (**Figure 6a**) only one peak pair (peak I) is displayed which is located near the potential value of peak I in $\text{Cu}_2\text{Zn}_2\text{SOD}$. In the CV diagram of $\text{E}_2\text{Zn}_2\text{SOD}$ (**Figure 6d**) peak I of $\text{Cu}_2\text{Zn}_2\text{SOD}$ disappeared due to the Cu(II) absence and the potential of peak II shifted slightly. The different shapes of the CV from **Figure 6c** and **6d** and the different capacitive currents suggest a difference in the adsorption properties of the copper and zinc derivatives. According to these experiments, peaks I and II were assigned to the reduction of Cu^{2+} and Zn^{2+} of $\text{Cu}_2\text{Zn}_2\text{SOD}$ respectively at the mercury electrodes surface despite the fact that quasi-reversible voltammetric peaks at potentials of approximately -0.6 V and in the region between -0.9 and -1.2 V (SCE) at pH 7 and at mercury electrodes are attributed to the reduction of disulphide bonds in the hydrophobic and in the hydrophilic region, respectively.

The DCP diagram obtained at DME (**Figure 7**) presents two well-defined waves with $E_{1/2}$ values -0.638 and -0.969 V , respectively. It was demonstrated that the first wave is due to the reversible one-electron reduction of Cu(II) and the second one to an irreversible two-electron reduction of Zn(II) in PESOD under steady state conditions. The overall process of PESOD was presented as follows:

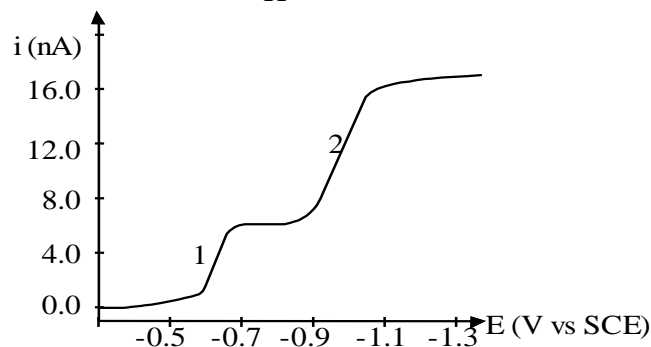
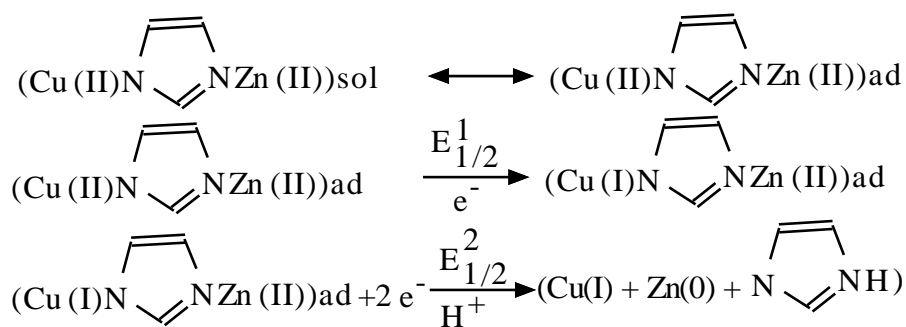
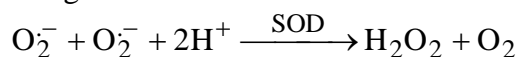


Figure 7. Direct current polarogram of PESOD (corrected for charging currents). 1. Cu(II)/Cu(I) couple. 2. Zn(II)/Zn(0) couple, concentration of PESOD is $1.8 \cdot 10^{-5} \text{ mol dm}^{-3}$ in 0.01 mol dm^{-3} phosphate buffer + 0.1 mol dm^{-3} KCl at pH 7.0, height of mercury column: 37.4 cm, flow rate of mercury drop: 1.15 mg s^{-1} , drop time: 4 s.

The protonation constant pK_a of the bridging imidazolite group of SOD was also calculated by using data of PESOD on mercury electrodes and the obtained value (7.85 ± 0.2) is in agreement with that obtained on other solid electrodes by using mediators [87]. The SOD activity was not lowered after reduction and re-oxidation which was confirmed using controlled potential electrolysis. [23]

SOD catalyses the following reaction:



and therefore it is useful in studying the participation of the radical in reactions involving oxygen such as autooxidations. The mechanism and kinetics of the autooxidation of pyrogallol was investigated by single-sweep oscillopolarography [88]. The electrochemical system of pyrogallol can also be employed to study the scavenging effect on O_2 and enzymatic determination. The role of O_2 in this reaction is investigated with the aid of SOD. Pyrogallol (1) reacts with dioxygen in weakly alkaline solutions to form purpurogallin (2) which then forms a blue transient species, thought to be the dianion of purpuroquinone (3) and then, via peroxide oxidation, species (4) (fig. 8). Single-sweep oscillopolarography shows that most intermediates and final products of reactions are electroactive substances. The autooxidation rate was considered as the initial rate of the peak current increasing at -0.20 ; -0.96 and -1.45 V vs. SCE.

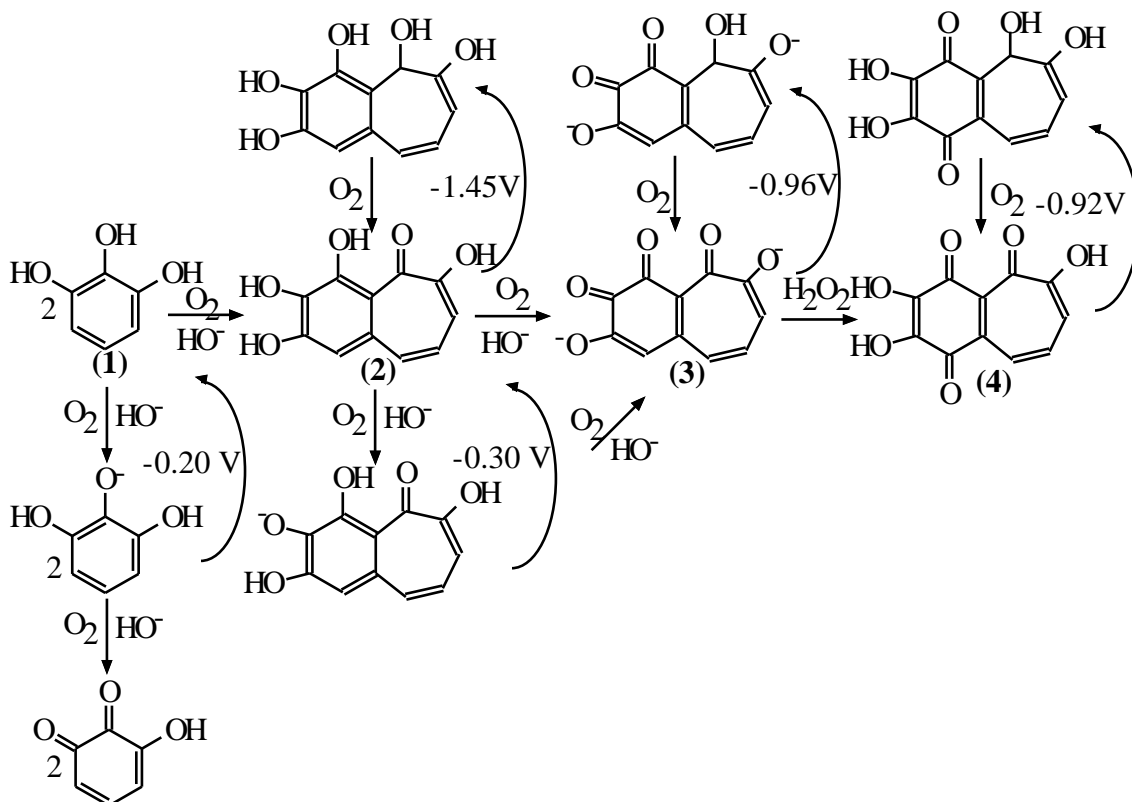


Figure 8. Reaction course scheme.

Pyrogallol autoxidation can be inhibited by SOD. The percent inhibition (I %) depends on both the quantity of SOD and the pH value. I % can be calculated according to the following equation:

$$I\% = \frac{h_0 h_1}{h_0} 100\% \quad (8)$$

where h_1 represents the average peak height in the presence of various concentrations of SOD and h_0 the average peak height in the absence of SOD.

The quantity of the enzyme inhibiting the reaction by 50 % (IC_{50}) is defined as one unit of SOD. This value can be calculated from **Figure 9**. DPV of xanthine in PBS solution in the absence (**Figure 10** curve b) and in the presence (**Figure 10**, curve c) presents an anodic oxidation peak at $E_{pa}=0.65$ V (**Figure 10**, curve b) and after XOD addition there appears a new oxidation peak at 0.15 V characteristic for the superoxide anion produced in the enzymatic reaction. In the absence of xanthine, XOD does not present any voltammetric response in the range 0-300 mV. Thus, the superoxide anion was further determined by

amperometry at 0.12 V although uric acid (the by-product of the xanthine oxidase reaction) can be oxidized at 0.20 V.

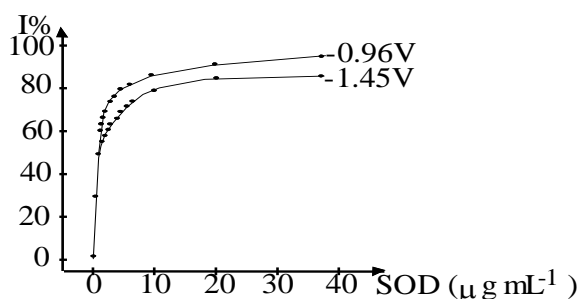


Figure 9. Inhibition of pyrogallol autoxidation by SOD. 0.20 mM pyrogallol in air equilibrated 45 mM tris-HCl buffer (pH 8.14) +1.00 mM DETA-PAC (diethylene triamine pentacetic acid). Scan rate: 300 mV s^{-1} ; $h(\text{square})=50 \text{ i}_p (\mu\text{A})$.

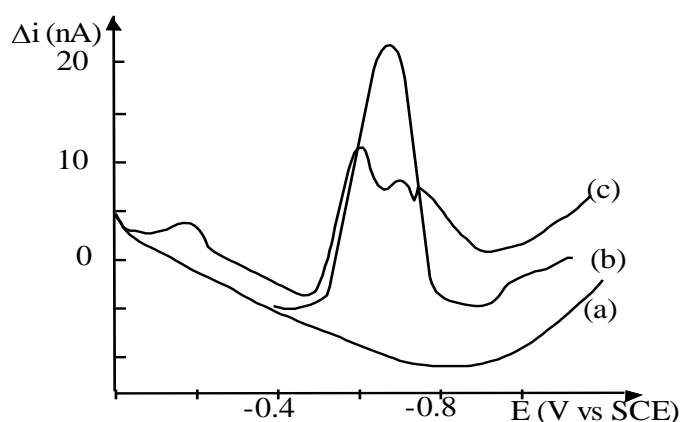


Figure 10. Differential pulse voltammogram of a bare carbon microfiber electrode in: curve (a) PBS (pH=7.4); curve (b) PBS + xanthine (240 μM); curve (c) PBS + xanthine (240 μM) + xanthine oxidase (0.2 μM). Experimental conditions: scan rate 20 mV s^{-1} ; $E_0=0 \text{ V}$; $E_{\text{pulse}}=50 \text{ mV}$; $\text{time}_{\text{pulse}}=40 \text{ ms}$; $\text{time}_{\text{pulse}}=60 \text{ ms}$.

Differential pulse voltammogram of xanthine recorded in PBS at a bare carbon

microelectrode at +0.12 V shows that after each XOD injection the current increases until it reaches a plateau corresponding to the kinetic equilibrium between the superoxide formation and its natural disproportionation [89]. The injection of SOD in the media results a current decreasing due to the acceleration of the superoxide disproportionation reaction.

The amperometric detection of the superoxide anion oxidation in the same conditions as above at 0.12 V was also demonstrated by the fact that the measured current increases after each KO_2 injections and is totally inhibited by the SOD addition. It was demonstrated that the amperometric current measured at 0.12 V is related to the superoxide anion oxidation without any effective interferences.

The quantification of superoxide production is difficult to be realised due to their natural and/or catalysed disproportionation by superoxide dismutase and because of their high reactivity towards other small molecules like nitric oxide [90-92]. Beside its important physiological functions NO acts as a destructive radical in the presence of superoxide anions (O_2^-) [90, 91] due to the formation of peroxy nitrates which are involved in many pathological pathways [93]. Several types of cells can produce simultaneously NO and O_2^- and thus it is important to follow simultaneously their production. Therefore, Privat et al. [94] have performed a direct electrochemical determination of both species production when they react with each others. For this purpose they used a bare carbon microelectrode for the amperometric detection of the superoxide anion and a NO-sensor for the amperometric detection of NO without any interference of the superoxide enzymatic reaction. The amperometric current recorded at 0.12 V for xanthine in PBS after XOD injections decreases immediately after NO addition proving that NO reacts quickly with superoxide generated in the electrochemical cell. The NO evolution at a NO-sensor was followed parallel with that of O_2^- at the bare carbon microelectrode. Immediately after NO injection the current evolves and then reaches a plateau that is proportional to the concentration of the free NO in solution near the electrode. After XOD addition O_2^- is produced and the current at the NO sensor decreases to reach the baseline value. This suggests that NO is consumed by O_2^- present in the solution due to the enzymatic reaction of xanthine with XOD.

Applications

Electrochemical sensors are of great interest due to their advantages, which include microfabrication and *in vivo* and *in vitro* applications [76]. The modification of transduction elements with enzymes would be an excellent method for preparing analytical devices, selective and efficient biomolecular recognition, by exploitation of specific and efficient enzyme-substrate reactivity. The hemoprotein cytochrome c undergoes facile reduction reaction with superoxide. SOD is a selective scavenger of superoxide and the best way for the detection of SOD thus could be the estimation of superoxide. Superoxide undergoes spontaneous disproportionation to produce H_2O_2 , an electroactive species. Thus, the electrical signal of the superoxide sensor system for interfering compounds is a very important limitation in its application.

Electrochemical sensors for the detection of superoxide radical could be developed by achieving electron transfer (ET) between the electrode and cyt c. Direct ET to cyt c modified electrodes surfaces has been well documented [63, 80-82] since the first reported from Taniguchi et al. in 1982 [59] and was used for electrochemical detection of O_2^- [67, 83-86, 96]. McNeil et al. utilised direct ET to solution dissolved cyt c at Au electrodes modified with 4,4'-dithiopyridine in the amperometric detection of O_2^- [83] and later reported the electrochemical detection of O_2^- by cyt c immobilised via N-acetylcysteine [84, 85]. The

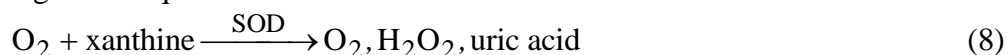
electrodes produced were used to measure directly the enzymatic and cellular production of the superoxide anion radical. The superoxide radical reduced the immobilised cyt c which was immediately re-oxidised by the surface modified gold electrode at a potential of +0.25 V (vs. Ag/AgCl). The electron transfer constant of this process was $3.4 \pm 1.2 \text{ s}^{-1}$. The rate of current generation was directly proportional to the rate of O_2^- production. This reagentless system was applied to the continuous monitoring of the free radical activity *in vivo* since oxygen derived free radical species act as mediators in inflammation diseases states [97]. Electrochemical sensors based on immobilised cyt c and SOD at different surfaces (surface modified gold-electrode and platinised activated carbon electrode-PACE) were used to measure the superoxide radical produced by stimulated neutrophils or by the system xanthine/xanthine oxidase. A biopsy needle probe electrode based on cyt c immobilised on PACE and suitable for continuous monitoring of free radical production was described [83].

The Au/HS(CH₂)₁₀COOH monolayer with surface immobilised cyt c was employed for the amperometric detection of the O_2^- anion [67, 86] and the long alkanethiol monolayer was reported to block the electrode surface [86]. However, because the physiological concentration of the superoxide anion is very low, the development of the efficient and fast-responding sensors is very important. In the performance of mediatorless sensors, the rate of the ET between the electrode and the immobilised probe molecule (enzyme, protein, etc.) will have an important role.

K. V. Gobi et al. [98] reported the direct electrochemistry of cyt c immobilised on Au-alkanethiolate monolayers and mixed-monolayers of 3-mercaptopropionic acid (MPA) with the coadsorbate, 3-mercaptopropanol (MP) and the electrochemical detection of O_2^- anion at cyt c-modified electrodes. The electrochemical characteristics and the superoxide anion sensor activities of cyt c immobilised on the monolayer and mixed-monolayer of MPA depend on the structure of the underlying alkanethiolate monolayer.

The CVs of cyt c bound to the monolayer of Au/MPA and Au/MPA+MP differ in two respects. First, E° of Au/MPA/cyt c (0.08 V) is approx. 100 mV more positive than that of Au/MPA+MP/cyt c (-0.01 V). Second, the ΔE_p at Au/MPA/cyt c is larger than that of Au/MPA+MP/cyt c. The surface density of the COOH groups at Au/MPA will be higher than that at Au/MPA+MP.

Both Au/MPA/cyt c and Au/MPA+MP/cyt c electrodes show anodic currents to O_2^- anion generated in-situ by enzymatic reaction of XOD with xanthine in oxygen-saturated solution according to the equation:



The response time was of ~ 15 s and the magnitude of the current response is higher at Au/MPA+MP/cyt c relative to that at Au/MPA/cyt c. During the generation of O_2^- , H_2O_2 and uric acid are produced in the electrolyte solution; catalase was added to the electrolyte solution to dissociate the coproduced H_2O_2 . The CV recorded during the generation of O_2^- anion shows an increase in the anodic peak with a decrease in the cathodic peak current. The observation of the increased anodic peak current with decreased cathodic peak current indicate that the O_2^- anion is oxidized electrocatalytically by cyt c but not at the bare electrode through pinholes, defect sites, etc. in the monolayer; the cyt c immobilised to the modified electrode is reduced by the O_2^- anion and the reduced cyt c is, then, oxidized electrochemically leading to the electrocatalytic oxidation of the O_2^- anion.

Among the two investigated cyt c-modified electrodes, Au/MPA+MP/cyt c showed a high anodic current for O_2^- anion and low interferences (of the H_2O_2 and uric acid coproduced in the enzymatic reaction). This electrode could be used for the detection of the O_2^- anion for

at least 5 days after the preparation.

Since the cyt *c*-modified electrodes respond immediately to different O_2^- anion levels in the electrolyte solution and give a steady state anodic current during the enzymatic generation of O_2^- anion, they could be used for the detection of SOD. The addition of the enzyme, which will rapidly dismutate the O_2^- anion into H_2O_2 and O_2 is expected to decrease the anodic current. The decrease of the steady-state current was directly proportional to the concentration of SOD added. The O_2^- sensor, Au/MPA+MP/cyt *c*, is very sensitive to the addition of SOD in the range of 10-800 mU mL⁻¹. Using the Au/MPA+MP/cyt *c* electrode a concentration of SOD in solution as low as 10 mU mL⁻¹ (~3 ng mL⁻¹) could be detected within a period of 1 min.

The same authors [99] performed amperometric detection of SOD with cyt *c* immobilised multilayer electrodes fabricated by forming a biopolymer membrane consisting of xanthine oxidase (XOD) and ascorbate oxidase (AOD) in poly-L-lysine, on the cyt *c*-immobilized mixed monolayer electrodes (Au/MPA+MP/cyt *c*). The resulted electrodes were denoted Au/cyt *c*/PL:(XOD,AOD). Au/cyt *c*/PL (XOD) electrode was prepared by excluding the addition of AOD. On Au/cyt *c*/PL:(XOD) electrode, AOD was immobilized using poly-L-lysine or without poly-L-lysine (using glutaraldehyde alone); the resulted electrodes were defined as Au/cyt *c*/PL:(XOD)/PL:(AOD) and Au/cyt *c*/PL:(XOD)/AOD_{glu}.

The activity of the cyt *c*-immobilized monolayer and multilayer electrodes for monitoring the superoxide generated by xanthine-XOD system was examined chronamperometrically at 0.15 V. While both the cyt *c*-immobilized monolayer and multilayer electrodes show anodic current responses to the generation of superoxide radical, the sensitivity of the multilayer system for the detection of superoxide radical was high relative to that of the monolayer system. In the case of the cyt *c*-multilayer electrodes, the generation of the superoxide radical near the sensing element, cyt *c*, resulted in high sensitivity for the detection of superoxide.

The presence of L-ascorbic acid, a potential scavenger of superoxide existing ubiquitously in the body, is to detriment for the detection of superoxide and SOD due to the reaction:



The cyt *c*-immobilized electrodes were examined for the detection of the superoxide radical in the presence of L-ascorbic acid. The use of a XOD and AOD-incorporated poly-L-lysine membrane enabled the detection of the generation of superoxide radical in the presence of L-ascorbic acid. The O_2^- radical generated in the biopolymer membrane would be electroanalytically oxidized by the immobilized cyt *c* giving an anodic current response. Superoxide radical diffusing out of the biopolymer membrane undergoes disproportionation, SOD-assisted dismutation and quenching with L-ascorbic acid and thus could not contribute to the amperometric response. The quenching of superoxide radical by L-ascorbic acid and SOD permeated into the membrane produces a current response. In the detection of SOD, the O_2^- radical generated by the XOD-xanthine enzymatic reaction in the biopolymer membrane will undergo a competitive reaction with cyt *c*, L-ascorbic acid and SOD. Au/cyt *c*/PL:(XOD, AOD) responds to the addition of SOD in the concentration range of 0.5 to 300 U mL⁻¹ and thus could be used for the detection of SOD as low as 0.5 mL⁻¹ in the presence of as much as 50 μM of L-ascorbic acid.

S. Mesaros et al. [100] developed an amperometric enzyme electrode for superoxide determination obtained by anodic polymerisation of pyrrole and concomitant incorporation of SOD on a Pt wire in phosphate buffer solution. The amperometric response to superoxide was measured at a potential of 0.7 V for the H_2O_2 oxidation. The response of the enzyme electrode

was rapid (3-5 s) and a linear relationship ($r=0.9988$) between current and the superoxide concentration was ranging in the 50-200 nM domain. A 15 nM detection limit was attained. The biosensor response was not affected by the presence of interference substances so that it can be used for measuring *in vivo* and in a single cell, respectively.

M. I. Song et al. [101] studied a trapping system for superoxide radical for the electrochemical detection of superoxide and the determination of superoxide generating enzymes like xanthine oxidase. The hypoxanthine-xanthine oxidase system was used to produce superoxide radical. The Teflon-membrane modified SOD electrode enabled a detection limit for hypoxanthine of 5 μ M. Teflon membrane placed in front of a Clark-type electrode reduces the interference of endogeneous hydrogen peroxide to 0.5 %.

A two channel sensor for simultaneous detection of superoxide radical and hydrogen peroxide in the concentration range 10^{-7} - 10^{-4} M consists of two glassy carbon microelectrodes covered by an electrodeposited polypyrrole/horseradish peroxidase (PPy/HRP) for H_2O_2 detection and by a composite membrane of SOD for the superoxide detection, respectively [102].

Acknowledgements: This work was supported by the CNFIS grant no.213/1999 and Matnantech grant no.65/2001.

REFERENCES

1. M. R. TARASEVICH, *Comprehensive Treatise of Electrochemistry*, Ed. S. Srinivasan, Y. A. CHIZMADZHEW, J. O'M. BOCKRES, B. E. CONWAY, and E. YEAGER, Plenum Press, New York, vol.10, p.231, 1985.
2. K. KANO, T. IKEDA, *Anal. Sci.*, **10**, 1013, (2000).
3. D. MELLER, J. T. Maloy, *Anal. Chem.*, **47**, 299, (1975).
4. J. K. LEYPOLDT, D. A. GOUGH, *Anal. Chem.*, **56**, 2896, (1984).
5. A. BERGEL, M. COMTAT, *Anal. Chem.*, **56**, 2904, (1984).
6. P. N. BARTLETT, R. G. WHITAKER, *J. Electroanal. Chem.*, **224**, 27, (1987).
7. P. N. BARTLETT, R. G. WHITAKER, *J. Electroanal. Chem.*, **224**, 37, (1987).
8. J. Y. LUCISANO, D. A. GOUGH, *Anal. Chem.*, **60**, 1272, (1988).
9. J. F. RUSLING, K. ITO, *Anal. Chim. Acta*, **252**, 23, (1991).
10. W. J. ALBERY, P. N. BARTLETT, B. J. DRISCOLL, R. B. LENNON, *J. Electroanal. Chem.*, **323**, 77, (1992).
11. F. BATTAGLINI, E. J. CALVO, *Anal. Chim. Acta.*, **258**, 151, (1992).
12. H. RANCHIAMAHAZAKA, J. M. NIGRETTO, *Electroanalysis*, **5**, 221, (1993).
13. N. MARTEBS, E. A. H. HALL. *Anal. Chem.*, **66**, 2763, (1994).
14. J. KONG, H. LIU, J. DENG, *Anal. Lett.*, **28**, 1339, (1995).
15. P. N. BARTLETT, K. F. E. PRATT, *J. Electroanal. Chem.*, **397**, 53, (1995).
16. P. N. BARTLETT, K. F. E. PRATT, *J. Electroanal. Chem.*, **397**, 61, (1995).
17. K. YOKOYAMA, Y. KAYANUMA, *Anal. Chem.*, **70**, 3368, (1998).
18. I. R. MILLER, in: G. MILAZZO, P. JONES, L. ROMPAZZO (Eds.), *Biological Aspects*

- of Electrochemistry*, Birkhauser, Basel, , p.477, 1971.
19. G. DRYHURST, K. M. KADISH, F. SCHELLER, R. RENNEBERG, *Biological Electrochemistry*, Academic Press, New York, 1982, p. 398.
 20. M. J. HONEYCHURCH, *Bioelectrochem. Bioenerg.*, **44**, 13, (1997).
 21. F. A. ARMOSTRONG, H. A. O. HILL, N. J. WALTON, *Acc. Chem. Res.*, **21**, 407, (1988).
 22. B. A. KUZNETSOW, G. P. SHUMAKOVICH, N. M. MESTECHKINA, *J. Electroanal. Chem.*, **248**, (1988).
 23. Z-WANG, W. QIAN, Q.-H. LUO, M-C. SHEN, *J. Electroanal. Chem.*, **482**, 8791, (2000).
 24. M. M. CORREIA DOS SANTOS, P. M. PAES DE SOUSA, M. L. SIMOES GONCALVES, H. LOPES, I. MOURA, J. J. G. MOURA, *J. Electroanal. Chem.*, **464**, 76, (1999).
 25. R.E. DICKERSON, R. TIMKOVICH in P. D. BOYER (ed.) *Enzymes*, 3rd edn., Academic Press, New York, vol.13, pp. 397, 1975.
 26. R. V. DUHALT, *J. Molec. Catal. B.: Enzymes*, **7**, 241, (1999).
 27. H. A. O. HILL, N. I. HUNT, *Methods in Enzymology*, cap. 19, vol. 227, Academic Press, NewYork, (1993).
 28. F. A. ARMSTRONG, J. N. BUTT, A. SUCHETA, *Methods in Enzymology*, Chapter 18, vol. 227, Academic Press, NewYork, (1993).
 29. R. SANTUCCI, M. BRUNORI, *Bioelectrochem. Bioenerg.*, **29**, 177, (1992).
 30. S. R. BETSO, M. H. KLAPPER, L. B. ANDERSON, *J. Am. Chem. Soc.*, **94**, 8197, (1972).
 31. F. SCHELLER, M. JANCHEN, G. ETZOLD, H. WILL, *Bioelectrochem. Bioenerg.*, **1**, 478, (1974).
 32. F. SCHELLER, M. JANCHEN, J. LAMPE, H. J. PRUMKE, J. BLANCK, E. PALECEK, *Biochem. Biophys.*, **412**, 157, (1975).
 33. F. SCHELLER, *Bioelectrochem. Bioenerg.*, **4**, 490, (1977).
 34. B. A. KUZNETSOW, N. M. MESTECHKINA, G. P. SHUMAKOVICH, *Bioelectrochem. Bioenerg.*, **4**,1, (1977).
 35. M. R. TARASEVICH, V. A. BOGDANOVSKAYA, *Bioelectrochem. Bioenerg.*, **3**, 589, (1976).
 36. T. M. COTTON, S. G. SCHULTZ, R. P. VAN DUYNE, *J. Am. Chem. Soc.*, **102**, 7960, (1980).
 37. W. R. HEINEMAN, B. J. NORRIS, J. F. GOELZ, *Anal. Chem.*, **47**, 79, (1975).
 38. M. J. EDDOWS, H. A. O. HILL, *Faraday Discuss. Chem. Soc.*, **74**, 331, (1982).
 39. M. J. EDDOWS, H. A. O. HILL, *J. Am. Chem. Soc.*, **101**, 4461, (1979).
 40. P. N. BARTLETT, J. FARINGTON, *J. Electroanal. Chem.*, **261**, 471, (1989).
 41. H. A. O. HILL, D. J. PAGE, N. J. Walton, *J. Electroanal. Chem.*, **217**, 141, (1987).

42. H. A. O. HILL, G. A. LAWRENCE, *J. Electroanal. Chem.*, **270**, 309, (1989).
43. I. TANIGUCHI, T. FUNATSU, M. ISEKI, H. YAMAGUCHI, K. YASUKOUCHI, *J. Electroanal. Chem.*, **193**, 295, (1985).
44. I. TANIGUCHI, N. HIGO, K. UMEKITA, K. YASUKOCHI, *J. Electroanal. Chem.*, **206**, 341, (1986).
45. J. E. FREW, H. A. O. HILL, *Eur. J. Biochem.*, **172**, 261, (1988).
46. M. BRUNORI, R. SANTUCCI, L. CAMPANELLA, G. TRANCHIDA, *Biochem. J.*, **264**, 301, (1989).
47. R. SANTUCCI, A. FARAONI, L. CAMPANELLA, G. TRANCHIDA, M. BRUNORI, *Biochem. J.*, **273**, 783, (1991).
48. K. B. KOLLER, F. M. HAWKRIDGE, *J. Electroanal. Chem.*, **2339**, 291, (1988).
49. M. A. HARMER, H. A. O. HILL, *J. Electroanal. Chem.*, **189**, 229, (1985).
50. J. HALADJIAN, P. BIANCO, P. A. SERRE, *Bioelectrochem. Bioenerg.*, **6**, 555, (1979).
51. B. A. KUTNESOV, G. P. SHUMAKOVICH, A. A. MUTUSKIN, *Bioelectrochem. Bioenerg.*, **14**, 347, (1985).
52. C. E. D. CHIDSEY, D. LOIACONO, *Langmuir*, **6**, 682, (1990).
53. J. M. SEVILLA, T. PINEDA, A. J. ROMAN, R. MADUENA, M. BLAZQUEZ, *J. Electroanal. Chem.*, **451**, 89, (1998).
54. T. LU, X. Yu, S. DONG, C. ZHON, S. YE, T. M. COTTON, *J. Electroanal. Chem.*, **369**, 79, (1994).
55. X. QU, J. CHOU, T. LU, S. SONG, C. ZHOU, T. M. COTTON, *J. Electroanal. Chem.*, **381**, 81, (1995).
56. C. CAI, *J. Electroanal. Chem.*, **393**, 119, (1995).
57. I. TANIGUCHI, M. ISEKI, K. TOYOSAWA, H. YAMAGUCHI, K. YASUKOUCHI, *J. Electroanal. Chem.*, **164**, 385, (1984).
58. I. TANIGUCHI, K. TOYOSAWA, H. YAMAGUCHI, K. YASUKOUCHI, *J. Electroanal. Chem.*, **140**, 187, (1982).
59. M. J. EDDOWES, H. A. O. HILL, *J. Chem. Soc., Chem. Commun.*, **21**, 771, (1977).
60. P. M. ALLEN, H. A. O. HILL, N. J. WALTON, *J. Electroanal. Chem.*, **178**, 69, (1984).
61. P. D. BARKER, K. DI GLERIA, H. A. O. HILL, V. J. LOWE, *Eur. J. Biochem.*, **190**, 171, (1990).
62. K. DI GLERIA, H. A. O. HILL, V. J. LOWE, D. J. PAGE, *J. Electroanal. Chem.*, **213**, 333, (1986).
63. P. YEH, T. KUWANA, *Chem. Lett.*, **1145**, (1977).
64. T. IKESHOJI, I. TANIGUCHI, F. HAWKRIDGE, *J. Electroanal. Chem.*, **270**, 297, (1989).
65. R. SANTUCCI, M. BRUNORI, L. CAMPANELLA, G. TRANCHIDA, *Bioelectrochem. Bioenerg.*, **29**, 177, (1992).
66. F. LISDAT, B. GE, F. W. SCHELLER, *Electrochem. Commun.*, **1**, 65, (1999).

67. W. JIN, U. WOLLENBERGER, F. BIER, A. MAKOWER, F. W. SCHELLER, *Bioelectrochem. Bioenerg.*, **39**, 221, (1996).
68. S. DONG, Q. CHI, *Bioelectrochem. Bioenerg.*, **29**, 237, (1992).
69. O. IKEDA, M. OHTAM, T. YAMAGUCHI, A. KOMURA, *Electrochim. Acta*, **43**, 833, (1998).
70. P. M. P. SOUSA, M. M. CORREIRA DOS SANTOS, M. L. SIMOES GONCALVES, *Port. Electrochim. Acta*, **15**, 407, (1997).
71. E. LOJOU, B. BIANCO, M. BRUSCHI, *Electrochim. Acta*, **43**, 2005, (1998).
72. E. LOJOU, B. BIANCO, M. BRUSCHI, *J. Electroanal. Chem.*, **452**, 167, (1998).
73. K. MIKI, T. IKEDA, H. KINOSHITA, *Electroanal.*, **6**, 703, (1994).
74. J. M. Mc CORD, I. FRIDOVICH, *J. Biol. Chem.*, **243**, 5753, (1968).
75. M. TARR, F. SAMSON, *Oxygen Free Radicals in Tissue Damage*, Birkhauser, Boston, (1993).
76. J. T. HANCOCK, *Br. J. Biomed. Sci.*, **54**, 38, (1997).
77. A. M. MICHELSON, J. M. Mc CORD, I. FRIDOVICH, *Superoxide and Superoxide Dismutase*, Academic Press, London, (1977).
78. D. K. DAS, N. MAULIK, *Methods Enzymol.*, **233**, 601, (1994).
79. Y. SATO, F. MIZUTANI, *J. Electroanal. Chem.*, **438**, 99, (1997).
80. M. J. TARLOV, E. F. BOWDEN, *J. Am. Chem. Soc.*, **113**, 1847, (1991).
81. M. COLLINSON, E. F. BOWDEN, M. J. Tarlov, *Langmuir*, **8**, 1247, (1992).
82. C. J. Mc NEIL, K. A. SMITH, P. BELLAVITE, J. V. BANNISTER, *Free Rad. Res. Commun.*, **7**, 89, (1989).
83. C. J. Mc NEIL, K. R. GREENOUGH, P. A. WEEKS, C. H. SELF, J. M. COOPER, *Free Rad. Res. Commun.*, **17**, 399, (1992).
84. J. M. COOPER, C. K. R. GREENOUGH, J. Mc NEIL, *J. Electroanal. Chem.*, **347**, 267, (1993).
85. F. LISDAT, B. Ge. E. E. FORSTER, F. W. SCHELLER, *Anal. Chem.*, **71**, 1359, (1999).
86. W. QIAN, Q.-H. LUO, M.-C. SHEN, *Bioelectrochem. Bioenerg.*, **39**, 291, (1996).
87. R. GAO, Z. YUAN, Z. ZHAO, X. GAO, *Bioelectrochem. Bioenerg.*, **45**, 41, (1998).
88. L. M. ELLERBY, D. E. CABELLI, J. A. GRADEN, J. S. VALENTINE, *J. Am. Chem. Soc.*, **118**, 6556, (1996).
89. J. S. BECKMAN, J. P. CROW, *Biochem. Soc. Trans.*, **21**, 330, (1993).
90. H. ISCHIROPOULOS, L. ZHU, J. S. BECKMAN, *Arch. Biochem. Biophys.*, **298**, 446, (1992).
91. J. P. CROW, J. S. BECKMAN, *Adv. Pharmacol.*, **34**, 17, (1995).
92. M. FEELISH, J. S. STAMLER (Eds.) *Methods in Nitric Oxide Research*, Wiley, New York, (1996).
93. C. PRIVAT, S. TREVIN, F. BEDIQUI, J. DEVYNCK, *J. Electroanal. Chem.*, **436**, 261, (1997).

94. P. MANNING, C. J. Mc NEIL, J. M. COOPER, E. W. HILLHOUSE, *Free Rad. Biol. Med.*, **24**, 1304, (1998).
95. W. SCHELLER, W. JIN, E. E. FOSTER, B. GE, F. LISDAT, R. BUTTEMEIER, U. WOLLENBERGER, F. W. SCHELLER, *Electroanalysis*, **11**, 703, (1999).
96. C. J. Mc NEIL, D. ATHEY, W. O. HO, *Biosens. Bioelectron.*, **10**, 75, (1995).
97. K. V. GOBI, F. MIZUTANI, *J. Electroanal. Chem.*, **484**, 172, (2000).
98. K. V. GOBI, F. MITZUTAMI, *Anal. Sci.*, **17**, 11, (2001).
99. S. MESAROS, Z. VANKOVA, S. GRUNFELD, A. MESAROSOVA, T. MALIMSKI, *Anal. Chim. Acta*, **358**, 27, (1998).
100. M. I. SONG, F. F. BIER, F. W. SCHELLER, *Bioelectrochem. Bioenerg.*, **38**, 419, (1995).
101. V. LVOVICH, A. SCHEELINE, *Anal. Chem.*, **69**, 454, (1997).